Biophysical Chemistry, 37 (1990) 43–59
Elsevier

BIOCHE 01464

A possible new control mechanism suggested by resonance Raman spectra from a deep ocean fish hemoglobin

Joel M. Friedman [a], Blair F. Campbell [a,*] and Robert W. Noble [b]

[a] *AT&T Bell Laboratories, Murray Hill, NJ 07974 and* [b] *Depts of Medicine and Biochemistry, SUNY at Buffalo, VA Medical Center, Buffalo, NY 14215, U.S.A.*

Received 22 January 1990
Accepted 1 February 1990

Ligand binding; Hemoglobin; Resonance Raman spectroscopy

The rattail fish, *Coryphaenoides armatus*, lives at ocean depths of 3000 m. As an adaptation for pumping oxygen into the swim bladder against the extreme pressures at the ocean bottom, the hemoglobin from this fish at low pH exhibits an extraordinarily low affinity for ligands. In this study, continuous wave and time-resolved Raman techniques are used to probe the binding site in this hemoglobin. The findings show an association between the low-affinity material and a highly strained heme-proximal histidine linkage. The transient Raman studies reveal differences in the protein structural dynamics at pH 6 and 8. The emerging picture derived from both this and earlier studies is that in vertebrate hemoglobins the heme-proximal histidine linkage represents a key channel through which species- and solution-dependent variations in the globin are communicated both statically and dynamically to the heme to produce an extensive range of ligand binding properties. Also presented is a new model that relates both intensity and frequency of the resonance Raman band involving the iron-proximal histidine stretching mode to specific protein controlled structural degrees of freedom. There emerges from this model a mechanism whereby modifications in the proximal heme pocket can further reduce the affinity of an already highly strained T state structure of hemoglobin.

1. Introduction

Genetic engineering has the potential of being at the center of future technologies based on custom modifications of both natural and synthetic protein structures. A relevant biophysical question is to what extent the variability in functional properties within a given class of proteins is controlled by well-defined tunable structural degrees of freedom. For example, most vertebrate hemoglobins bear a striking resemblance to each other. From one organism to the next, they all have the same oxygen-binding heme chromophore and the same overall protein morphology. Despite the structural similarities, the functional properties can vary dramatically from one species to the next. Furthermore, for a given hemoglobin the reactivity towards oxygen displays a strong dependence upon solution conditions. The initial question as applied to hemoglobin translates into whether these species- and solution-dependent changes in reactivity arise through many different, perhaps unrelated, structural channels or through some specific or limited number of structural degrees of freedom that can be tuned by either evolution, genetic engineering or solution conditions to give rise to the broad range of observed oxygen-binding properties.

An approach to this problem is to examine the structure of many different hemoglobins for the purpose of correlating specific structural features with relevant functional properties. This approach

Correspondence (present) address: J.M. Friedman, Chemistry Dept, New York University, New York, NY 10003, U.S.A.
* Present address: Aerodyne Corp., Los Angeles, CA, U.S.A.

is facilitated by examining those materials that are at extreme end points of reactivity, i.e., exceedingly low- or high-affinity hemoglobins for the case at hand. In this context, the hemoglobin from the deep-sea rattail fish *Coryphaenoides armatus* (C.a.) was chosen for study. At low pH, half of the heme groups of this hemoglobin exhibit what is perhaps the lowest ligand affinity for any vertebrate hemoglobin [1].

The results of a recent comparative study [1] of the ligand binding properties of hemoglobins from *C. armatus* and other deep-sea fishes were interpreted in terms of two heterogeneous binding sites. At low pH in the presence of inositol hexaphosphate (IHP), a P_{50} for CO of 100 mmHg at 15 °C was measured for the low-affinity sites on the hemoglobin *C. armatus*. Assuming a partition coefficient of 100, this would suggest a P_{50} for O_2 of some 13 atm. This extraordinarily low affinity for CO arises primarily from a very slow 'on' rate (approx. 10^2-times slower than for 'normal' deoxyhemoglobins). At high pH, the on rate still has a slow component that is almost an order of magnitude slower than typical deoxyhemoglobin (unpublished results). It is suggested that the exceptional ligand binding properties of this hemoglobin are related to the functional requirement of pumping oxygen into the oxygen-rich gas phase of the swimbladder of this fish at the abyssal depths ($\sim$ 3000 m) at which it is found.

In this study, resonance Raman spectroscopy is used to probe the local environment at the ligand binding site in Hb(C.a.) as a function of solution conditions (pH and IHP) and degree of ligand saturation. Earlier studies [2–6] indicate that the ligand-free ferrous heme is responsive to variations in the protein structure; consequently, all comparisons made in this study are among deoxyhemes surrounded by either equilibrium or nonequilibrium protein structures. The latter structures are generated using short laser pulses both to photodissociate the initial liganded material and to generate the resonance Raman spectrum of the deoxyheme surrounded by and hence influenced by the as yet unrelaxed protein structure of the starting liganded species [7]. This approach allows us to compare the ligand binding site of the deoxy and liganded hemoglobin as a function of solution conditions. In all cases, it is the protein structure that is the variable altering the spectrum of the deoxyheme. The results of this Raman study reveal that at the heme there are only slight frequency differences between normal deoxyhemoglobins and deoxy-Hb derived from *C. armatus*. There is, however, a dramatic difference in the relative resonance enhancement of the Raman band corresponding to the iron-proximal histidine stretching mode ν(Fe-His). An analysis of the relationship between the frequency and the relative intensity of ν(Fe-His) in the resonance Raman spectrum leads to a detailed microscopic model that connects structure, spectra and function. This model includes several novel features which suggest strategies, both natural and synthetic, by which extremely low ligand binding affinities can be generated.

2. Materials and methods

The fish were obtained during two expeditions aboard the R/V Oceanus as described previously [1]. The procedures for both the collection of the blood and the subsequent preparation of purified hemoglobin solutions were as previously described [1].

The paucity and scant availability of material necessitated the use of a microvolume rotating Raman cell into which was placed a fraction of a 1 ml volume of sample ($\sim 10^{-4}$ M heme). A rubber septum allowed for a controlled atmosphere about the sample. Spectra of equilibrium species and near-steady-state populations were generated with approx. 20–30 mW of 441.6 nm excitations (Liconix, He-Cd laser). The spectra of the nonequilibrium deoxy species occurring within 10 ns of photodissociating either the oxy or carboxy derivative were generated with a 10 ns pulse at approx. 441.6 nm from an excimer laser-pumped dye laser (Lambda Physik) operating at 25 Hz ($\sim$ 1 mJ/pulse). The back-scattered radiation was collected and then dispersed by a 0.64 m single spectrograph (I.S.A. 640, with a 2400 groove/mm grating) and detected on an intensified reticon multichannel detector (Princeton Instruments, IRY 700). Samples were run at ambient temperatures.

3. Results

3.1. Deoxyhemoglobin as a function of pH

The high (1300–1650 cm^{-1}) and low (150–400 cm^{-1}) frequency Raman spectra of deoxy-Hb (*C. armatus*) showed little superficial variation with solution conditions. The detectable differences between samples at pH 8.5 (100 mM Cl^-, 10 mM Tris) and at pH 6.0 (100 mM Cl^-, Bistris) occurred in two inversely correlated modes [2,5,8]; ν_4, at approx. 1355 cm^{-1} and ν(Fe-His), the iron-proximal histidine stretching mode, at approx. 215 cm^{-1}. Relative to the high-pH sample, the low-pH sample exhibits a ν_4 that is shifted approx. 1 cm^{-1} to higher frequencies and a ν(Fe-His) that is shifted to lower frequencies by approx. 3 cm^{-1}. The presence of IHP (1.5 mM) did not alter the spectra of the low-pH sample. The low-frequency spectra are shown in fig. 1. Also shown in fig. 1 for comparison purposes is the corresponding spectrum of adult human deoxyhemoglobin (HbA). The spectrum of deoxy-HbA is invariant with respect to these pH changes. The peak frequency of ν(Fe-His) is the same for deoxy-HbA and the pH 8.5 deoxy-Hb (*C. armatus*) sample. A striking difference is seen in the relative intensity of ν(Fe-His). For HbA, ν(Fe-His) is a little more than half the intensity of the 366 cm^{-1} band, whereas for Hb(C.a.) both at high and low pH, ν(Fe-His) is more than twice the intensity of the 366 cm^{-1} band. Other Raman bands from *C. armatus* samples which are derived primarily from porphyrin motions displayed roughly the same relative intensities (with respect to each other including the 366 cm^{-1} reference band) as for deoxy-HbA.

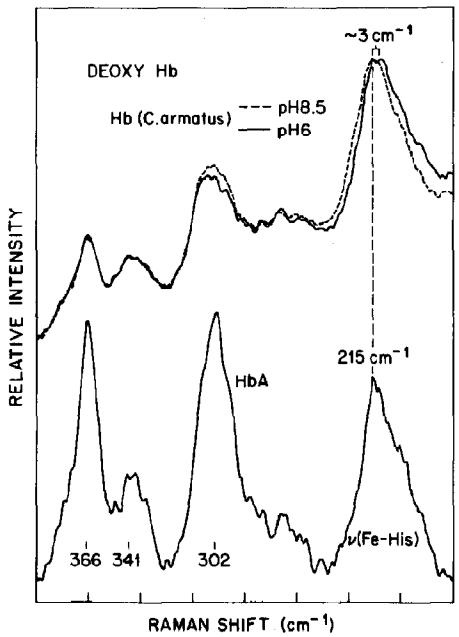

Fig. 1. Comparison of low-frequency resonance Raman spectra of deoxyhemoglobins.

3.2. Photoproducts of carboxy forms of Hb(C.a.)

A spectral comparison of nonequilibrium deoxyhemoglobins is shown in fig. 2. It can be seen that the deoxy transient generated within 10 ns of photodissociating CO-Hb(C.a.) yields roughly the same spectrum under high- and low-pH (+IHP) conditions. Compared to the respective equilibrium deoxy spectra (fig. 1) both nanosecond spectra show two key features. The distinct 341 cm^{-1} peak observed for the equilibrium species is replaced by a broadening on the low-frequency side of the 366 cm^{-1} band and the frequencies for ν(Fe-His) of the 10 ns photoproduct are relative to the stable deoxy species, increased by approx. 3 and 6 cm^{-1} for the high- and low-pH samples, respectively. It should be noted that the end-point value for ν(Fe-His) is very nearly the same for both high- and low-pH transient species. Also shown in fig. 2 are the spectra of the near-steady-state populations of photoproduct generated during the 10–50 μs illumination window created by the combination of rotating sample cell and clear white laser. For the high-pH sample (C), the 366–341 cm^{-1} region appears intermediate between the stable deoxy form and the 10 ns photoproduct. The frequency of ν(Fe-His) is still the same as for the nanosecond transient (i.e., 3 cm^{-1} higher than that of high-pH deoxy-Hb at equilibrium). The low-pH sample (D) yields a spectrum that is identical to that of the corresponding low-pH equilibrium deoxy-Hb sample. The spectrum of the low-pH sample was unaffected by either the presence or absence of IHP or the rate of rotation

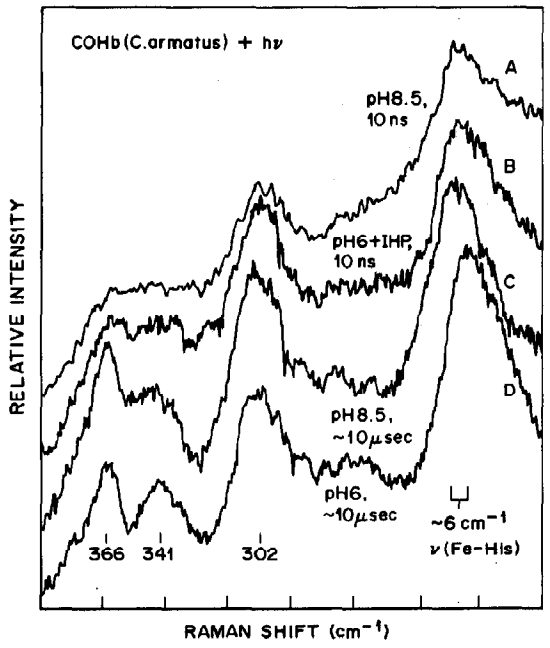

Fig. 2. Comparison of the resonance Raman spectra of the deoxy photoproduct of photodissociated carboxyhemoglobins. (A) 10 ns photoproduct, pH 8.5; (B) 10 ns photoproduct at pH 6.0+IHP; (C) approx. 10 μs photoproduct, pH 8.5; (D) approx. 10 μs photoproduct spectrum at pH 6.0+IHP.

(0–30 rev. s^{-1}). The lack of material precluded a more detailed pulse probe time-resolved study.

3.3. Oxy-Hb(C.a.) at pH 6.0

Hb(C.a.) at pH 6.0 in the presence of oxygen at normal pressures remains half saturated [1]. Fig. 3 shows the ν_4 Raman mode for such a sample under fast and slow rotation conditions for the spinning cell. Under conditions of fast rotation, the ν_4 region contains both a deoxy and oxy band, whereas slow-rotation conditions yield a spectrum with a marked reduction in the oxy peak. Since the deoxy and oxy forms of Hb have different Soret band absorption peaks, the resonance enhancement for the 441.6 nm excitation is different for these two derivatives. Based on the similarity between the absorption spectra of Hb(C.a.) and those of other hemoglobins and on the resonance Raman excitation profiles of heme-proteins [9], we conclude that the spectrum from the rapidly rotating cell is consistent with a half-oxygenated sample.

Fig. 4 depicts the low-frequency spectra of both the fast (F) and slowly (S) rotating samples as well as a fully deoxy sample at the same low pH. The slow-spin sample yields a low-frequency spectrum that is very nearly identical with that of the pH 6.0 deoxy-Hb(C.a.) sample. The frequency, intensity and line shape of ν(Fe-His) are the same in these two cases. At high rotational speeds the spectrum of the oxy sample changes. As can be seen in fig. 4, ν(Fe-His) for the fast rotating cell is at a higher peak Raman frequency (~ 215 vs 212 cm^{-1} for deoxy), considerably narrower and much more intense compared to deoxy-Hb(C.a.). The quantity and stability of the sample prevented our obtaining an interpretable 10 ns photoproduct spectrum of the half-saturated oxy material.

3.4. Summary of experimental results

Table 1 contains a summary of the frequencies observed for ν(Fe-His) as a function of solution conditions for Hb(C.a.). As shown (in parentheses) are designations to indicate the relative intensity of ν(Fe-His). Included for comparison purposes are values for HbA, Hb(tuna), Hb(Kempsey)

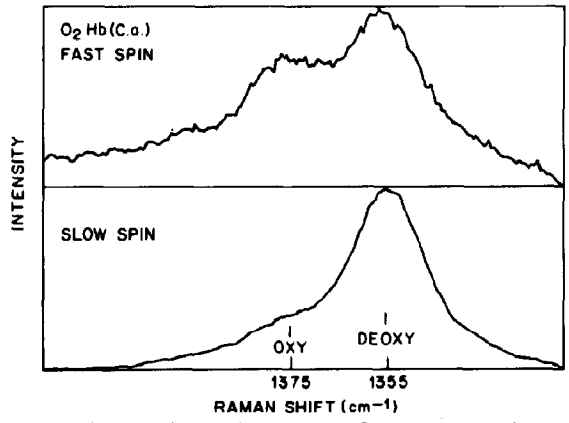

Fig. 3. The ν_4 region of the resonance Raman spectra of a pH 6.0 sample of Hb(C.a.) in the presence of oxygen under ordinary pressure conditions in a rotating cell at fast and at slow rotational speeds. The frequency of the ν_4 band can be used to distinguish five- from six-coordinate ferrous hemes as indicated by the arrows.

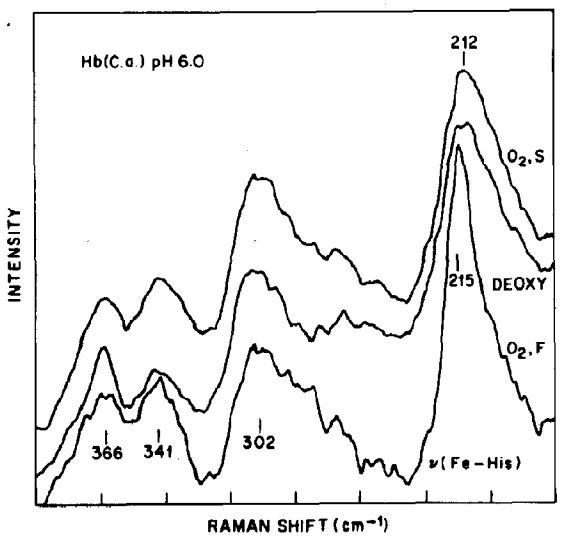

Fig. 4. Low-frequency resonance Raman spectra of the same fast (F) and slowly (S) rotating pH 6.0 partially oxygenated sample used to generate fig. 3.

and Mb. The key distinguishing features of Hb(C.a.) with respect to most other vertebrate hemoglobins are: (1) The shift in the frequency of ν(Fe-His) for deoxy-Hb(C.a.) from a normal T-state value of approx. 215 cm^{-1} at pH 8 to the extremely low value of 212 cm^{-1} at pH 6.0.

Table 1

Frequency (in cm^{-1}) of ν(Fe-His) for equilibrium and transient (deoxy*) forms of deoxyhemoglobins and myoglobin

Values of other hemoglobins and Mb are taken from refs 2, 3, 13, 18 and 36. The designations W, M, S and VS, which refer to the relative intensity of ν(Fe-His) compared to the relatively invariant approx. 366 cm^{-1} band, correspond to weak, medium, strong and very strong, respectively.

	Deoxy	Deoxy* (10 ns)	Deoxy* (>1 μs)
Hb(C.a., pH 6.0)	212 (S)	222 (S)	212 (S)
Hb(C.a., pH 6.0 + IHP)	212 (S)	222 (S)	212 (S)
Hb(C.a., pH 8.5)	215 (S)	222 (S)	222 (S)
Hb(C.a., pH 6.0 + O_2)	216 (VS)		212 (S)
Hb(A, pH 6 + IHP)	215 (W)	226 (S)	< 222 (W)
Hb(A, pH 8.5)	215 (W)	230 (S)	> 222 (M)
Hb(Kempsey, pH 9.0)	220 (W)	230 (S)	
Hb(tuna, pH 7.5)	216 (M)	228 (S)	
Mb	222	222	222

(2) The enhanced intensity of ν(Fe-His) for the deoxy form.
(3) Both high- and low-pH forms of COHb(C.a.) have identical 10 ns photoproduct spectra despite being functionally very distinct.
(4) The half-liganded (oxy) low-pH form has a ν(Fe-His) for the deoxy sites that is sharper, more intense and higher in frequency than the corresponding fully deoxy sample.

4. Discussion

In the previous sections, it was shown that the resonance Raman spectra of different forms of Hb(C.a.) exhibit distinctive features. Obvious questions which stem from these observations include:
(1) What is the structural basis for these distinctive spectral features?
(2) To what extent do these features account for or reflect the extreme functional properties of Hb(C.a.)?
(3) How do these features and their associated (if any) functional significance fit into the current schemes used to explain the structural basis for hemoglobin reactivity?

In the following sections we shall attempt to address these questions. We will first explore the structural basis for the intensity and frequency behavior of ν(Fe-His) and then attempt to integrate the structural and dynamical information contained within the Raman spectra into a comprehensive model to account for the functional properties of vertebrate hemoglobins.

4.1. Spectra and structure

Detailed structural comparisons among a broad spectrum of functionally disparate species and/or states of hemoglobin would be ideally accomplished using high-resolution X-ray crystallographic techniques [10]. Unfortunately, that technique has severe constraints that limit its applicability. Insofar as the resonance Raman bands from hemoglobin can be assigned to vibrations of specific structural degrees of freedom, Raman spectroscopy provides a more facile probe of the local structure about the ligand-binding site. The

iron-proximal histidine stretching mode is one of the better characterized [3,5,6] features in the Soret enhanced Raman spectrum of five-coordinate high-spin heme forms of hemoglobin and myoglobin. The behavior and properties of this mode as reflected in the resonance Raman spectra of the various forms of Hb(C.a.) indicate that Hb(C.a.) is not only at an extreme end-point for functional properties of hemoglobin but is also similarly extreme in the structure that determines the properties of ν(Fe-His). Since the iron-proximal histidine linkage has been implicated in the control of hemoglobin reactivity, it is important to consider the origin of the ν(Fe-His) features in the Hb(C.a.) spectra both as a possible explanation for the functional properties of Hb(C.a.) and as a means of exploring the range of control mechanisms within hemoglobins in general. Several studies [3,5,6] have exposed relationships between frequency of ν(Fe-His) and both the structure and functionality of the probed population. The present study raises the prospect that the relative intensity of ν(Fe-His) may also be relatable to functional properties. This idea is further supported by results obtained from cryogenic studies on myoglobin photoproducts. The temperature dependence of ν(Fe-His) from the photoproduct of CO-Mb shows a progressive increase in the intensity of ν(Fe-His) in going from 2 to 200 K [5,11,12]. The frequency, however, does not begin to shift until above 100 K (Friedman, unpublished results), suggesting that intensity and frequency are not obligatorily coupled. Optical pumping of fully photodissociated CO-Mb samples at 4 K and higher temperatures induces an increase in the intensity of ν(Fe-His) but not a change in the frequency [13]. It was shown that such optical pumping also causes a slowing in the rebinding kinetics [14]. Thus, a possible connection exists between increased ν(Fe-His) intensity (relative to heme modes) and decreased rates of rebinding. This idea is additionally supported by our observation that the slowest rebinding population of photodissociated O_2-Mb has a higher intensity ν(Fe-His) than the corresponding fully photodissociated CO-Mb sample at all temperatures between 2 and 80 K. (Friedman unpublished results, and ref. 14).

In order to compose a structural picture that accounts for both frequency and intensity of ν(Fe-His) in the Hb(C.a.) spectra, it is necessary to have a model which relates differences in those parameters with variations in some specific structural degree of freedom. In the subsequent sections, we first review an earlier model that deals just with the frequency of ν(Fe-His) and then develop a new and more comprehensive model that includes intensity as well. With this model it is then possible to begin addressing the issue of the structural basis for Hb(C.a.) reactivity.

4.1.1. ν(Fe-His) and structure: frequency

The Raman frequency of the ν(Fe-His) mode is an indication of the effective bond strength of the iron-histidine linkage: the lower the frequency the weaker the bond. Variations in this frequency with protein structure are claimed to be a direct measure of protein-induced strain between the proximal histidine and the heme. The variation in frequency has been attributed to the F-helix-induced tilt of the histidine with respect to the heme plane (or a shift of the heme with respect to the F-helix) [3,5,7,15]. It is postulated that an increase in the protein-induced tilt results in a weakening of the Fe–histidine bond due to an increase in the nonbonding repulsive interaction between the heme atoms and the nearest imidazole carbon. The detailed X-ray picture suggests that there may in fact be a constellation of protein-induced steric influences aside from the tilt that can further modify the heme-histidine interaction [10]. The frequency of ν(Fe-His) remains nonetheless an overall indicator of the net effective bond strength between the heme and the histidine for the five-coordinate Fe^{2+} systems.

4.1.2. ν(Fe-His) and structure: Raman intensity

The ν(Fe-His) band exhibits species and structure-dependent variations not only in frequency [2–8, 16–20] but also in its relative intensity even for a given frequency. Excitation profile studies of ν(Fe-His) show that this mode is resonantly enhanced through Soret band excitations [9]. This enhancement pattern indicates a coupling of the π-electron systems of the heme and the imidazole. Thus, the resonance enhancement of ν(Fe-His)

depends upon three factors: (1) coupling of the imidazole electronic and vibrational motions to the heme; (2) the homogeneous and inhomogeneous contributions to the width of the resonant optical transition; (3) the relative offset of the resonance excitation from the peak of the resonance. Several arguments can be given as to why only the first is likely to be the primary factor responsible for the difference in the relative intensity of ν(Fe-His) between Hb(C.a.) and other hemoglobins. Since there are no sizable differences among absorption spectra from the various species of deoxy-Hb it is not at all likely that there are large enough differences in the optical widths to cause species-specific differences in the resonance Raman damping factors. Such an effect has been observed in cytochromes [21] but in this case there occur discernible differences in the absorption line shapes. Furthermore, since both the heme modes and the iron-histidine stretching mode are enhanced through the same optical transition, variations in the electronic damping constant should not preferentially influence one of these modes over the others. Similarly, given the comparable absorption spectra and the common Soret enhancement mechanism for ν(Fe-His) and certain heme modes [9], it is not very plausible to explain large species-specific variations in the relative intensity of ν(Fe-His) in terms of differences in the offset from resonance. Since it is ν(Fe-His) alone which displays the large variation in relative intensity and since for the reasons given above factors (2) and (3) are not likely to be contributory, we focus upon the electronic coupling between the imidazole of F8 and the heme as the cause of this intensity variation. The known variability in the relative orientation of the F8 imidazole and the heme makes this casual relationship all the more plausible.

Champion and co-workers [9] have proposed an enhancement model based upon the interaction of the σ^*(Fe-N_{His}) and π^* porphyrin orbitals [9]. In this model, the variations in both the frequency and intensity of ν(Fe-His) stems from the coupling of the σ^*(Fe-N_{His}) and π^* porphyrin orbitals. The coupling of these orbitals is a function of the iron displacement, tilt angle (θ) and azimuthal angle (ϕ) (see fig. 5). Although this

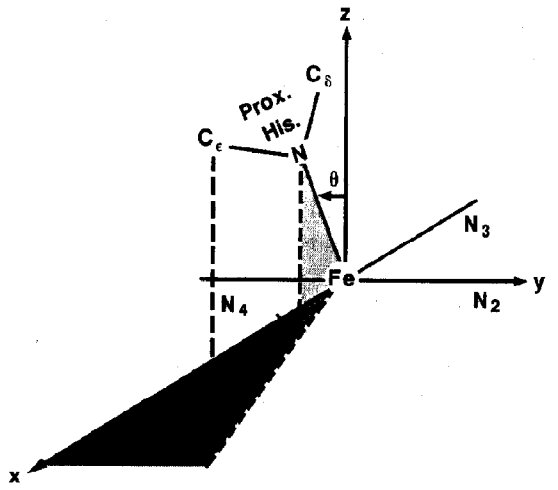

Fig. 5. Angular coordinates defining the relative position of the proximal histidine and the heme macrocycle. C_ϵ and C_δ, histidine carbon atoms; N_1–N_4, heme pyrrole ring nitrogens. The angle θ defines the tilt of the histidine from the heme normal and the angle ϕ denotes the rotation of the projection of the histidine on the porphyrin plane with respect to the N(1)–Fe–N(3) axis.

hypothesis has been used to account for several Raman observations, including the behavior of ν(Fe-His) in the cryogenically trapped photoproduct of CO-Mb [10], it also has implications that are problematic. The most significant such problem is the implied close relationship between the frequency and intensity of ν(Fe-His) which arises from the same orbital coupling mechanism contributing to both observables. As seen in the present work, the intensity and frequency are not obligatorily coupled.

An alternative hypothesis relating geometry to ν(Fe-His) intensity is derived from the extended Hückel calculations of Scheidt and Chipman [22]. They showed that for protein-free iron porphyrins the observed azimuthal angle ϕ could result from a balance between steric interactions (favoring a large ϕ) and π interactions between the iron and the imidazole (favoring the eclipsed $\phi = 0°$ configuration). Since the iron-imidazole bond is predominantly of σ character, its strength (and hence the frequency of ν(Fe-His)) would not be significantly affected by variations in ϕ. On the other hand, the Soret band resonance enhancement of ν(Fe-His) should be sensitive to variations in ϕ

insofar as it reflects the variation in π overlap between the iron and the imidazole. Consequently, in comparisons of systems having nearly the same frequency for ν(Fe-His), variations in the intensity of ν(Fe-His) are to be attributed to variations in ϕ. Structures having high intensity for ν(Fe-His) are therefore assigned a smaller value for ϕ relative to similar structures exhibiting lower intensity for ν(Fe-His). Changes in the displacement of the iron from the heme plane are also expected to influence the π overlap that determines the intensity of ν(Fe-His). Since the displacement should be responsive to changes in the tilt angle θ, comparison between hemoglobins having different ν(Fe-His) values can show differences in the intensity of ν(Fe-His) due to different combinations of rotation and iron displacement.

4.1.3. Tilt, rotation and iron displacement: separate but connected degrees of freedom

The above model leads to a clear separation between the factors contributing to the intensity and frequency of ν(Fe-His). The frequency of ν(Fe-His) is taken as a direct measure of the influence of proximal strain upon the iron-histidine bond strength and the intensity of ν(Fe-His) is a reflection of the protein modulated (vide infra) value for the azimuthal angle ϕ. The X-ray crystallographic data from various hemoglobin and myoglobin derivatives reveal trends that connect the various parameters capable of influencing ν(Fe-His) [10]. Both the X-ray and EXAFS [23] studies indicate that for five-coordinate species, structures having lower frequencies for ν(Fe-His) (e.g., T vis-à-vis R deoxy-Hb) have larger displacements of the iron out of the heme plane. Karplus and co-workers [24] have shown for hemoglobin that the architecture of the proximal heme pocket imposes a preferred value for ϕ. Changes in specific protein- and heme-related coordinates can result in changes in the protein-specific 'preferred' value of ϕ. In HbA and Mb where ϕ has a range of accessible values, greater values of ϕ are associated with both larger values of θ and small or no displacement of the iron from the heme plane. Steric repulsion can be increased by either increasing the tilt angle θ or having the iron more in plane. The tilt angle and the iron displacement are also correlated in that larger tilts are associated with greater iron displacements (possibly being reflected in the sterically weakened iron–imidazole bond). We now propose the following picture relating ν(Fe-His) and key structural elements associated with assorted proximal strain models for hemoglobin reactivity (e.g., see refs 3, 24 and 33):

(1) The frequency of ν(Fe-His) in equilibrium and transient forms of Hb and Mb is a *reflection* of protein-induced proximal strain: the lower the frequency the greater the strain.
(2) In the X-ray crystallographic data, the F-helix-mediated proximal strain for deoxy heme-protein species is reflected in the tilt angle θ, the displacement of the iron from the heme plane and the related pyrrole nitrogen–imidazole carbon distances.
(3) Soret band excitations result in structure-dependent resonant enhancements for ν(Fe-His) that depend upon electronic interactions between the imidazole and the iron. This predominantly π interaction is modulated primarily through variations in the azimuthal angle ϕ and probably to some lesser degree through variations in the above parameters connected with proximal strain.
(4) The parameters of proximal strain (θ and the iron displacement) and ϕ are interrelated in that for a given θ a more out of plane iron is associated with a smaller ϕ and for a given displacement of the iron a larger θ (increased tilt) favors a larger ϕ.

The above proposed interplay among spectral and structural parameters is summarized in fig. 6. The shaded area represents a distribution of values for ϕ based on a recent [25] kinetic hole-burning study [26] from which it is concluded that for a given tilt angle θ there is a distribution of rotational angles ϕ with an accompanying distribution of iron displacements. Fig. 6 shows how the distribution shifts towards larger values of ϕ with increasing θ. It should be emphasized at this point that a given spectral value such as the frequency or intensity of ν(Fe-His) represents an

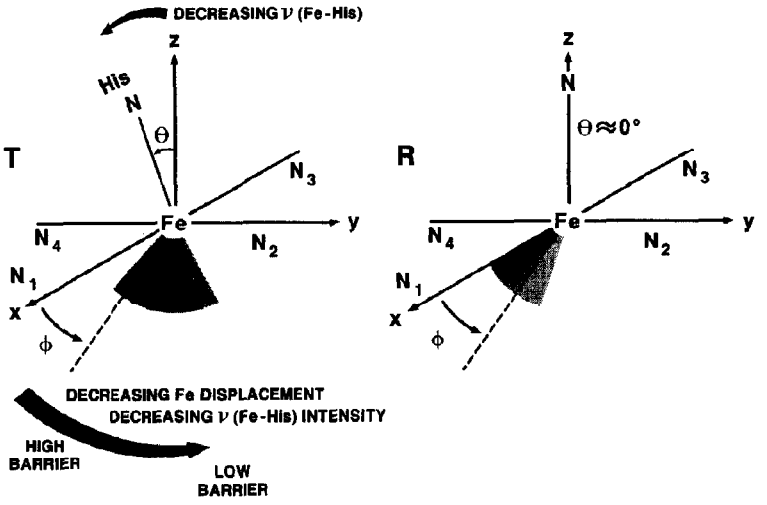

Fig. 6. A schematic showing the interplay among structural and spectral parameters. In going from the left to the right, χ decreases as occurs in tertiary structure changes associated with the T-to-R transitions. As a result of the decrease in nonbonding repulsive interactions between the histidine and the heme upon decreasing θ, ϕ can adopt a more eclipsed conformation provided this movement is not constrained by the architecture of the proximal heme pocket. The rotational parameter ϕ is represented as a distribution in ϕ (see text). Associated with the distribution in ϕ is a distribution in the iron displacement. Thus, for a given θ which is imposed largely by the allosteric core [24] there is a linked distribution in both ϕ and the iron displacement with the distribution of ϕ limited by the architecture of the heme pocket. The structures having the lowest ligand-binding affinity would have a large θ (low ν(Fe-His)) overall tertiary structure and be a member of the distribution of conformational substates that has a small ϕ and a large iron displacement. Deoxy-Hb(C.a.) appears to have both a large ϕ and, unlike other T-state deoxy forms, a heme pocket that constrains ϕ to low values.

average value for some distribution of conformational substates.

4.2. HbA

The Raman spectrum of deoxy-HbA shown in fig. 1 illustrates several key features. The 341–366 cm^{-1} region contains two well-defined peaks that are the hallmark for the tertiary structure associated with the heme pocket of an equilibrium deoxy-Hb for either the R or T quaternary state [3,4]. Both low relative intensity and the 215 cm^{-1} frequency for ν(Fe-His) are characteristic of mammalian T-state deoxyhemoglobins. It has recently been shown that these deoxy T-state features are invariant over a series of T-state mutant and chemically modified human deoxyhemoglobins [19]. Within the framework of the above model, the low frequency and low intensity of ν(Fe-His) for deoxy-HbA stems from a tilted (large θ), rotated (large ϕ) histidine with an enhanced displacement of the iron out of the heme plane. In contrast to deoxy-HbA, the R-state photoproduct (10 ns) of liganded HbA (CO, O_2 or NO) exhibits a ν(Fe-His) with both higher frequency 230 cm^{-1} and greater relative intensity [3,4,15]. The deoxy R forms of HbA (using either Hb(Kempsey) or the 1–5 μs transient photoproduct of CO-HbA at pH $\leq$ 7.0) have values for ν(Fe-His) that are intermediate (222 ± 3 cm^{-1}) between those of the deoxy T and the 10 ns R-state photoproduct. These results are consistent with the existence of a progression in the coupled degrees of freedom involving the iron-histidine linkage in going from deoxy T to deoxy R to liganded R for HbA. The structural picture based on the analysis of the Raman spectra is one in which the decrease in tilt in going from deoxy T to deoxy R to R-state photoproduct is also coupled to a decrease in azimuthal angle of the histidine and in the displacement of the iron.

4.3. Hb(C.a.)

Unlike the situation for HbA, ν(Fe-His) for the deoxy form of Hb(C.a.) shifts with decreasing pH from a typical T-state value (215 cm^{-1}) to an even lower frequency. The observation that at pH 8 the frequency for deoxy-Hb(C.a.) is equivalent to that of deoxy-HbA implies a standard deoxy T-state value for the heme-histidine bond; however, the lowered frequency at pH 6 indicates an even weaker or more strained bond ('super' T state?). The spectra from deoxy-Hb (*C. armatus*) are unusual not only because of this evidence for enhanced proximal strain at low pH but also because of the intensity pattern for ν(Fe-His). The spectra of both the high- and low-pH forms of deoxy-Hb (*C. armatus*) differ dramatically from other deoxyhemoglobin spectra in that the relative intensity of ν(Fe-His) is significantly greater for the former spectra. Within the context of the above discussion, the increased intensity of ν(Fe-His) could be due to a proximal heme pocket that constrains ϕ to low values and prevents the usual rotation in response to the highly tilted T-state heme-histidine geometry (as reflected in the low frequencies for ν(Fe-His)). A heme-histidine geometry with a near zero rotation has an increased π overlap between the heme and the histidine which results in a greater relative resonance enhancement of ν(Fe-His). This configuration has implications for reactivity as is discussed in section 4.5. Since the intensity for ν(Fe-His) does not vary with changes in frequency and since the observed frequency at pH 8 is the same as for most other T-state deoxyhemoglobins, it is unlikely that the anomalously high intensity of ν(Fe-His) for Hb(C.a.) originates from an atypical displacement of the iron. This conclusion follows because the frequency of ν(Fe-His) should also be highly responsive to shifts in the iron displacement. It would appear that for all of these T-state deoxy forms the iron probably is at the extreme limits for being out of the heme plane.

The low-pH form of Hb(C.a.) in the presence of O_2 at sub-hyperbaric pressures appears to be half-saturated [1]. The high-frequency spectrum of such an oxy sample in a rotating cell spun at high speed (which minimizes photodissociation) is consistent with only half the binding sites being occupied. At slower rotation speeds, the sample exhibits spectral evidence of substantial photodissociation and manifests the equilibrium deoxy low-frequency Raman spectra. The low-frequency spectrum of the unbound sites in the half-saturated sample reveals a ν(Fe-His) that is substantially sharper and more intense than for the fully deoxy sample. This narrower band is also at higher frequency than the broad band for the fully deoxy sample. An unambiguous analysis of this result is not possible because it is not established whether or not the binding of O_2 at two of the four binding sites induces a tertiary structural change that influences the unbound sites. In either case, the observed deoxy-heme spectrum reflects the structure of the low-affinity sites; nonetheless, it needs to be determined whether this contributing structure is the same as that which contributes to the spectrum of the fully deoxy material. Clarification of this issue would be achieved by generating the 10 ns photoproduct spectrum of the half-liganded species and comparing it to the fully deoxy spectrum. Unfortunately, the sample stability and quantity thwarted our attempts in this direction. However, it does look as though the ν(Fe-His) of the half-saturated sample is the result of the loss of the less-intense lower frequency component of the composite spectrum from the fully deoxy sample. In this case, the pH 6.0 deoxy spectrum is made up of an intense band at approx. 215 cm^{-1} and a much less intense band at lower frequency. This interpretation implicates the more intense 215 cm^{-1} band as belonging to the subunits with the anomalously low affinity for O_2. Based on the presented model relating structure to the properties of ν(Fe-His), the low-affinity subunit in the low-pH sample would have a histidine tilt somewhat greater than the β-subunit of deoxy-HbA (215 vs 218 cm^{-1}) but with the additional key feature of having a much more eclipsed (small ϕ) heme-histidine conformation. This combination for Hb(C.a.) produces a weaker σ bond and greater π overlap relative to the β-subunit of HbA. Extending this interpretation to the higher pH deoxy-Hb(C.a.) sample, we contend that the frequencies of the α- and β-subunits are similar to those of deoxy-HbA but the intensity of the β-

subunit continues to remain anomalously high for the former sample. Thus, the major difference in going from high to low pH for deoxy-Hb(C.a.) is a shift to lower frequency for ν(Fe-His) in the β-subunits without a change in relative intensity. The assignment of the unusual subunit in Hb(C.a.) to the β-class is based solely on these spectral comparisons, since no structural data exist.

4.4. Structural relaxation

The Raman spectra of the deoxy-like photoproduct of CO-Hb(C.a.) at 10 ns subsequent to photodissociation show that ligand binding induces persistent tertiary structure changes in the protein under conditions where the protein both is and is not cooperative (pH 8 and pH 6 + IHP, respectively). This protein should be contrasted with myoglobin where spectral evidence indicates a loss of ligation-induced structural features in the photoproduct within at most a few picoseconds [27–29]. Persistent (> 10 ns) ligation-induced tertiary changes [18] are, however, the rule for hemoglobins including noncooperative structures having either low affinity (Hb(Kansas) [7]) or high affinity (Hb(Tuatara) [16], Hb(Kempsey) [31]). What is unusual in the case at hand is that the high- and low- (with and without IHP) pH carboxy samples both have essentially the same 10 ns photoproduct spectrum. The steady-state spectra taken with a rotating cell show that at low pH the relaxation to the equilibrium deoxy T state occurs faster than approx. 10 μs whereas at high pH the population shows very little if any relaxation over this time window. These findings indicate that in spite of nearly identical local heme-heme pocket conformations in the early time photoproducts, the photoproducts' relaxation time is strongly solution dependent. As observed earlier for HbA [30], low-pH conditions favor faster tertiary relaxation of the initial photoproduct. The tertiary structure relaxation of the T-state photoproduct of CO-Hb (tuna, *Thunnus thynnus*) at pH 6 was observed to occur within 1 μs whereas the R^- state photoproduct of CO-HbA at high pH shows very little relaxation over this time scale [30].

4.5. Structure and reactivity

The above analysis of the Raman data can now be used as a basis for an understanding of the functional properties of Hb(C.a.). Our goal is to explore systematically the functional implications of our structural picture in order to see if any of the elements of this picture are likely to be the cause of the exceptional functional properties of Hb(C.a.). We first consider the potential role of both the histidine tilt and rotation in the control of reactivity. We then examine whether these control mechanisms are likely to be operational in Hb(C.a.) and to what extent Hb(C.a.) fits into the overall pattern of control within vertebrate hemoglobins.

4.5.1. Proximal strain and the energetics of ligand binding: the frequency of ν(Fe-His) as an indicator of the protein spring constant

The systematic variations in ν(Fe-His) for both transient and stable *deoxy* species of hemoglobin indicate a corresponding systematic variation in the Fe-His bond strength. Despite the fact that for deoxyhemoglobins the different quaternary and tertiary structures exhibit varying degrees of strain in this bond (as reflected in ν(Fe-His)) [32], the energies associated with these differences do not appear to be of sufficient magnitude to account for variations in reactivity among the different structures [33]. Nonetheless, these small differences in the deoxy structures do imply differences in the ligand-bound structures that account for functional differences.

Each value of ν(Fe-His) implies a configuration of the heme-histidine linkage for the probed deoxy species. Low frequencies of ν(Fe-His) indicate a tilted (or 'strained') configuration; however, the out of heme plane displacement of the iron minimizes the repulsive interactions between the imidazole and the heme. Based on picosecond Raman studies [27,34], it is concluded [5,31,34] that, to a first approximation, those structural elements (including histidine F8 and segments of the F helix) between the iron and the $\alpha_1\beta_2$ interface can be viewed as a tight spring with a protein-tunable spring constant (see fig. 7). Movement of iron is coupled to this spring. The configuration and sta-

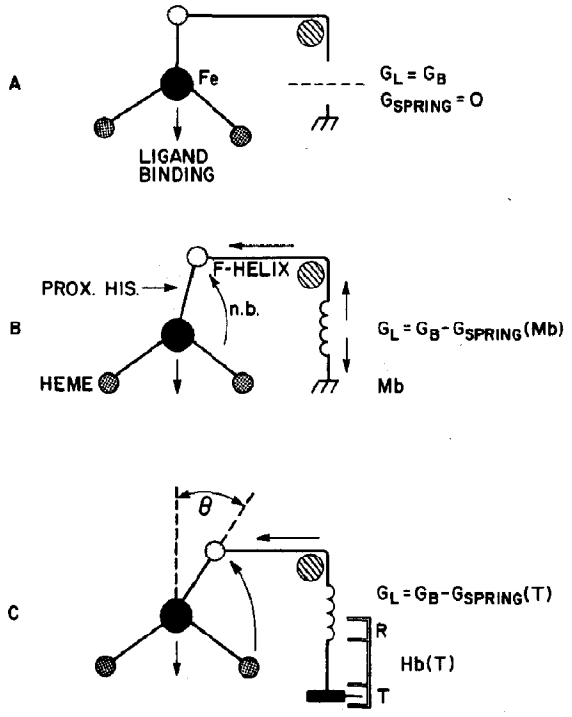

Fig. 7. A schematic of the spring model description of the proximal strain contribution to ligand binding. In the absence of any proximal restraint (A), the drop in free energy upon ligand binding G_L is equal to G_B. In cases B and C, the movement of the iron into the heme plane requires the additional work (G_{spring}) of straightening the proximal histidine ($\theta \rightarrow 0°$) against the pull of the F-helix spring. In the case of myoglobin (B), the anchoring of the spring is to a fixed structure, whereas in hemoglobins (C), there are switchable anchor points which correspond to the R and T configurations of the $\alpha_1\beta_2$ interface. The spring constant of the F helix is set by the $\alpha_1\beta_2$ interface. As the iron moves into the heme plane, the nonbonding repulsive interaction (n.b.) increases, generating the torque that straightens the proximal histidine (Prox. His.). The free energy lost from G_B through G_{spring} is available to drive structural rearrangements such as the T → R transition which modifies the spring ($G_{spring}(T) \rightarrow G_{spring}(R)$).

bility of the $\alpha_1\beta_2$ interface have been shown to control the static and dynamic properties of ν(Fe-His) [3,15,30]. Thus, the interface can be viewed as the element controlling the set point for the tilt of the proximal histidine. The tilt determines the nonbonding (denoted by n.b. in fig. 7) repulsive interactions between the heme and the histidine. This tilt-modulated interaction both contributes to the above spring constant and modifies the displacement of the iron (the greater the tilt the greater the nonbonding repulsive interaction with the heme and the larger the displacement of the iron from the heme plane in the five-coordinate case). The key point is that the frequency for ν(Fe-His) indicates or reflects a specific spring constant (or distribution of spring constants). The lower the frequency of ν(Fe-His) the greater is the spring constant.

In the case of myoglobin at ambient temperatures where equilibrium deoxy-Mb and the deoxy photoproduct at 30 ps have the same frequency for ν(Fe-His) [27], the protein structure and the spring constant are minimally changed by ligand binding and solution conditions. In contrast, hemoglobin exhibits ligand- and solution-dependent quaternary and tertiary structure changes that indicate considerable tunability of the spring constant.

The proposed direct connection between the frequency of ν(Fe-His) in the five-coordinate species and the spring constant for the movement of iron provides a direct link between structure and function. Maximum stability for the iron-ligand bond is a six-coordinate heme system in which the iron is in the plane of the heme. Raman and infrared studies show that in solution both R and T forms of at least some liganded hemoglobins have the same local, in-plane configuration at the iron [35,36]. To achieve this configuration upon ligand binding requires that the iron move from an out-of-plane to an in-plane configuration. Since the spring constant (as reflected in ν(Fe-His) in the starting five-coordinate species) is a function of quaternary and tertiary structure, different structures will require different amounts of energy to move the iron in plane. A key point is that the iron-histidine bond is not the relevant spring, but rather, the changes in the iron-histidine bond strength (as reflected in the Raman spectra) are indications of changes in the overall spring that does dictate the energetics of moving the iron in plane.

Calculations show that the repulsive interactions between the imidazole carbons and the pyrrole nitrogens increase as the iron moves into the heme plane [36–38]. A tilted histidine substantially increases the repulsive interaction especially

when the iron is only slightly out of the heme plane. It has been postulated that the absence of R-T differences in the spectroscopic indicators of local structure at the iron for six-coordinate species in solutions indicates that as the iron goes in plane the repulsive interactions increase sufficiently to become the dominant local interactions, [3,4,20,23]. The net result is that in solution for most hemoglobin structures the repulsive interactions for the *in-plane iron* are sufficient to keep the histidine upright regardless of the magnitude of the tilt-inducing forces from the $\alpha_1\beta_2$ interface. Thus, as shown in fig. 7, in comparing five-coordinate systems that are unconstrained and untilted to ones that are constrained and tilted, the movement of the iron from an out-of-plane to an in-plane position requires for the latter the added work of straightening up the histidine against the pull from the interface (G_{spring} in fig. 7). The pull on the 'F helix spring' which both straightens the histidine ($\theta \rightarrow 0°$) and transmits state of ligation information to the interface is generated by the increase in the nonbonding interaction as the iron moves into the heme plane. This iron-generated torque on the histidine is represented in fig. 7 as a curved arrow extending from the heme through the line representing the tilted histidine. Champion and co-workers [33] have recently taken a major step in making aspects of this model more quantitative.

The extra low T-state frequency for ν(Fe-His) from deoxy-Hb(C.a.) at pH 6 (with and without IHP) indicates an enhanced tilt or strain from the heme histidine configuration and hence a larger G_{spring} for the movement of the iron into the heme plane. Based on the proposed relationship between the frequency of ν(Fe-His) and the spring constant controlling ligand binding, one would expect that if there were no other factors controlling reactivity, then for the pH 6 sample, the subunit having the lowest frequency would have the lowest ligand affinity. The intense, narrowed ν(Fe-His) band at 215 cm^{-1} for the partially oxygenated pH 6 Hb(C.a.) sample strongly implies that the oxygen binds to the subunit having the lower frequency. This result raises the issue of what other factors might influence the reactivity. Assuming that the higher frequency component of deoxy-Hb(C.a.) has the low affinity, we consider how it differs from deoxy-HbA. Studies on iron-metal hybrid hemoglobins show that the β-subunit of deoxy-HbA has a ν(Fe-His) at 218 cm^{-1} and is less intense than the 266 cm^{-1} band [5,6,20]. The results on the half-oxygenated sample suggest that the low-affinity 'β'-subunit in Hb(C.a.) at low pH is, relative to the β-subunit in deoxy-HbA, slightly lower in frequency (215 vs 218 cm^{-1}) and very much more intense. Although this reduction in frequency for the β-subunit of Hb(C.a.) should lower the oxygen affinity (all other things being equal) relative to the HbA β-subunit, it seems likely that additional factors contribute to the dramatically reduced O_2 affinity. This point is further strengthened from the results at high pH where the frequency of ν(Fe-His) is the same for deoxy-Hb (C.a.) and deoxy-HbA and yet the former still displays a markedly reduced ligand on-rate for CO compared to HbA (R. Noble, unpublished data). The enhanced relative intensity of the ν(Fe-His) for the β-subunit is a reasonable focus for the additional factor.

4.5.2. Histidine rotation and ligand reactivity

The substantially greater intensity of ν(Fe-His) for the β-subunit of deoxy-Hb(C.a.) compared to that of HbA indicates, within the framework of our analysis, that the Hb(C.a.) histidine is in a more eclipsed orientation. The nonbonding interactions between the pyrrole nitrogens and the eclipsing carbons of the tilted imidazole ring should make moving the iron into the heme plane energetically more costly than for a comparable geometry that differs only in being less eclipsed. Since smaller values for the azimuthal angle should enhance the repulsive interactions arising from the above-mentioned nonbonding interactions, the spring constant for the allosteric core should also depend upon ϕ especially when accompanied by a large tilt angle θ. Thus, the spring constant and G_{spring} can be modulated by both the tilt and rotation of the heme-histidine unit. Protein control of the spring constant can therefore occur both by varying the stability of the $\alpha_1\beta_2$ interface which most directly influences the histidine tilt and by modifying the proximal pocket so as to constrain the proximal histidine at a specific rota-

tional angle ϕ.

4.5.3. Strategies for a low-affinity hemoglobin

Studies on iron-cobalt hybrid hemoglobin show that for HbA a switch from the T state to the R state is facilitated more by ligand binding to the β-subunit over the α-subunits [39,40]. A reasonable strategy for generating a low-affinity hemoglobin that still retains the same basic 'machinery' as other vertebrate hemoglobins (such as HbA) is both to stabilize the T structure and to decrease the affinity of the β-subunit. The general lowering of the frequency of ν(Fe-His) for deoxy-Hb(C.a.) at pH 6 is a strong indication of an exaggerated or extreme T-like $\alpha_1\beta_2$ interface. The low frequency of ν(Fe-His) for the early photoproduct of CO-Hb(C.a.) suggests enhanced stability of a T-like interface. An enhanced intensity for ν(Fe-His) in Hb(C.a.) regardless of ν(Fe-His) frequency and solution conditions suggests that the proximal pocket has been modified to restrict tightly the proximal histidine to more eclipsed configuration. At low pH, the combination of an increased tilt (lower ν(Fe-His)) and a decrease in azimuthal angle (higher ν(Fe-His) intensity) for the β-subunit of deoxy-Hb(C.a.) might ensure that the α-subunit preferentially binds O_2, thereby minimizing the destabilization of the T state by ligand binding.

4.5.4. Structure, dynamics and reactivity

The changes in ν(Fe-His) at both low and high pH in going from the stable deoxy species to the 10 ns transient photoproduct indicate that even when under noncooperative ligand-binding conditions, there are at least two tertiary structures necessary for understanding the equilibrium and kinetics of reaction of this hemoglobin with ligands. The increased frequency of ν(Fe-His) for the low-pH photoproduct relative to the starting deoxy species suggests that the presence of the ligand shifts the conformational equilibrium of the protein toward more 'normal' geometries. It is intriguing that the frequencies of ν(Fe-His) for the high- and low-pH photoproducts (10 ns) are very nearly the same despite different reaction equilibrium and kinetics. If we make the plausible assumption that solution-dependent differences in the reactivity of this hemoglobin all originate from variations in proximal constraints, then the question arises as to how the same initial proximal structures as reflected by ν(Fe-His) values yield different ligand kinetics. An answer is suggested from the observation (fig. 2) that although the initial spectra of the 10 ns transients are nearly the same, the microsecond transient populations are radically different. The low-pH sample has a microsecond spectrum that resembles the low-pH deoxy sample, whereas the high-pH sample more closely resembles the initial photoproduct. The microsecond results suggest that solution conditions modulate the relaxation times for tertiary structures which are coupled to the heme histidine linkage. This result in turn suggests a modulation of equilibrium among relevant tertiary structures. The Raman data reveal three tertiary structures designated χ_1, χ_2, χ_3 in fig. 7. In the absence of ligand, χ_1 and χ_2 predominate at low- and high-pH, respectively, whereas in the presence of excess ligand, χ_3 predominates at both high and low pH. The Raman kinetic data imply that by increasing the pH of the solution in the presence of excess ligand, the stability of χ_3 is still further enhanced over that of χ_1 and χ_2. Thus, for a solution containing excess ligand at equilibrium, χ_3 is overwhelmingly the most populous species at both high and low pH; nevertheless, the low-pH sample will contain more of the minority species (χ_1 and χ_2).

It is of interest to consider first how local structure at the heme influences the elemental steps that contribute to the macroscopic parameters of reactivity. Two key steps are the intrinsic rate of iron-ligand dissociation and the ligand-binding rate from within the heme pocket. The latter is the final step in any ligand-binding process. It has been designated by Frauenfelder and co-workers [41] as process I. Variations in the yield of geminate recombination are in most instances controlled by this final step [3,5,15,40,42–44]. As a direct consequence of the proposed tight spring-like coupling between the iron and the determinants of quaternary structure (vide supra), the heights of potential energy barriers for both spontaneous dissociation and geminate recombination are functionally related to the iron-prox-

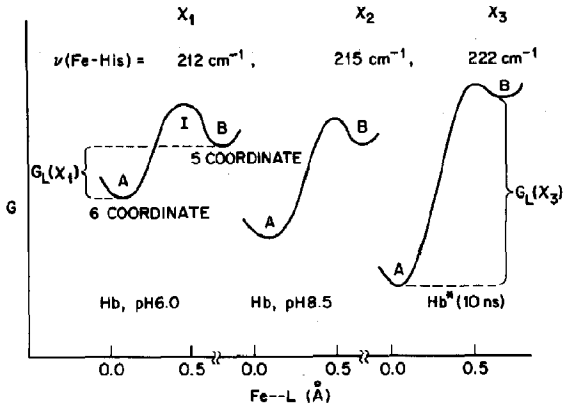

Fig. 8. A schematic of possible reaction coordinate diagrams detailing the changes in free energy (G) upon ligand binding and protein structural relaxations. The protein coordinate χ is some combination of allosteric components that define the functionally relevant tertiary and quaternary structure of the protein (i.e., heme, histidine F8, F-helix FG corner, etc.). Also shown is the proposed relationship between χ, $G(\chi)$ and the frequency of the iron-proximal histidine stretching mode ν(Fe-His).

imal histidine linkage (see figs 6–8). In many instances for a large variety of vertebrate hemoglobins, changes in solution conditions that alter ν(Fe-His) in the photoproduct spectra also change the yield of geminate recombination and probably the rate of spontaneous dissociation. A rough correlation exists showing that a solution- or species-induced shift to lower frequencies for ν(Fe-His) is accompanied by a decrease in the yield of geminate recombination consistent with an increase in the innermost barrier for process I [3,5,31,40,42,44]. A quantitative study of the geminate process for carboxy derivatives of metal hybrid forms of HbA shows that this innermost barrier is what modulates the nanosecond geminate process in going from the R to the T states of HbA [43]. Since the barriers controlling geminate recombination and dissociation are also key elements in the full description of ligand on- and off-rates, it is not surprising that a correlation with ν(Fe-His) extends to these macroscopic parameters of reactivity as well [40,44]. Lower frequencies appear to correspond to structures that exhibit lower reactivity. The emerging picture is that a value for ν(Fe-His) for a given structure dictates the proximal strain (spring constant) contribution to the barriers controlling reactivity.

Applying the picture to χ_1–χ_3 leads to the qualitative picture shown in fig. 8, where the barrier for spontaneous dissociation increases and that for geminate recombination decreases in going from χ_1 to χ_2 to χ_3. The structural relaxations which follow photolysis and exhibit variable relaxation times suggest that the extrapolation from the kinetics of geminate processes to an understanding of ligand affinity may be complex, especially if the geminate processes precede the relaxation in the structure of the local heme pocket or occur during this relaxation. The reason is simply that the population of deoxy conformers which result from photolysis must in general be quite unlike the population which results from spontaneous ligand dissociation at equilibrium. To conclude otherwise is to postulate that at equilibrium different conformational states are involved in ligand binding and dissociation. This, however, requires that at equilibrium the binding and dissociation reactions occur by different pathways, a condition that violates the requirement of microscopic reversibility. Instead, the rates of ligand dissociation from the many conformers will vary, perhaps widely, reflecting differences in their ligand affinities and these rates along with the relative concentrations of the various conformers will define the population of states formed by spontaneous dissociation, whereas the photodissociation experiments are typically dominated by only the most populous conformational species. For the case at hand as shown in fig. 8, each of the conformational populations, defined as χ_1, χ_2 and χ_3 on the basis of ν(Fe-His), has a particular spontaneous dissociation constant and geminate rebinding rate. The overall measured off-rate is a product of the intrinsic bond rupture rate times the probability that the ligand does not undergo geminate recombination. The 10 ns transient Raman data show that χ_3 predominates at equilibrium in the presence of excess ligand. If, however, the off-rate for χ_3 is very low whereas for χ_1 or χ_2 it is high, then the major pathway for dissociation and relaxation at equilibrium may be the very low population of ligand-bound χ_1 or χ_2. In the transient experiments only the properties of

χ_3 are probed. The similarity in the 10 ns photoproducts at low and high pH indicates that in the presence of the ligand, χ_3 conformers dominate the equilibrium under both conditions. One must realize, however, that the rate of ligand dissociation from this set of conformers may be vanishingly small as suggested in fig. 8. Instead, as discussed above, dissociation may occur predominately from a conformer which is present in very small amounts but from which ligand dissociates rapidly. The overall rate of spontaneous dissociation would then be controlled by the concentration of the population of this conformer, a concentration which could vary widely with pH and still remain undetected in the population of the 10 ns photoproduct. The pH dependence of the structural relaxation observed in the Raman spectra is consistent with such a change in equilibrium populations. This is not to say that ν(Fe-His) of the photolysis product is without interest. It appears to reflect the affinity of ligand binding to the conformer which predominates in the liganded state. This is one of the critical parameters in the overall equation for the free energy change associated with ligand binding to the deoxygenated molecule.

5. Summary

The hemoglobin from the deep ocean fish *C. armatus* has an extremely low ligand binding affinity. For CO it has been shown [1] that at low pH the low affinity arises largely from an on-rate that is two orders of magnitude lower than for normal T-state deoxyhemoglobins. Increasing the pH increases the on-rate by only a factor of seven. In the present study, an attempt is made to understand the origin of the low affinity through a resonance Raman study of the heme environment in high- and low-pH forms of deoxy-Hb(C.a.), half-saturated Hb(C.a.) and photodissociated CO-Hb(C.a.). For the deoxy samples, the most visible difference in the Raman spectra between HbA and Hb(C.a.) occurs in ν(Fe-His), the iron-proximal histidine stretching mode. Whereas at pH 8, deoxy-Hb(C.a.) exhibits the same frequency for ν(Fe-His) as deoxy-HbA, the low-pH deoxy-Hb(C.a.) is shifted to a lower frequency by 3 cm^{-1} relative to HbA and high-pH Hb(C.a.). At both pH values, the Raman spectra of deoxy-Hb(C.a.) are strikingly different from those of other deoxy-Hb samples in that the relative intensity of ν(Fe-His) to the heme modes is substantially greater. A connection between the relative resonance enhancement of ν(Fe-His) and reactivity is made not only from Hb(C.a.) but also from cryogenic Raman studies on both optically pumped CO-Mb photoproducts and Mb photoproducts derived from different ligand-bound species. In the attempt to understand the connection between spectra and function, a model is developed in which the relative intensity of ν(Fe-His) is modulated by variations in the azimuthal angle between the imidazole of F8 and the iron-pyrrole nitrogen axis. The azimuthal angle modulates the π-electron coupling between the heme and the histidine. A discussion is presented that both relates the histidine tilt and rotation to each other and to iron displacement and connects these Raman detectable structural parameters to ligand binding reactivity. The resulting picture, in conjunction with data on Hb(C.a.) half-saturated with O_2, suggests natural and synthetic strategies for developing ultra low-affinity hemoglobins.

A discussion is also given on the relationship of the transient Raman data to the kinetic parameters associated with equilibrium measurements.

Acknowledgements

This work was partially supported by NSF (DMB8604435) (J.M.F.), and by research funds from the Veterans Administration and USPHS Grant HL 12524 from the National Heart, Lung and Blood Institute and NIH Program Project P01-HL40453.

References

1 R.W. Noble, L.D. Kwiatkowski, A. DeYoung, B.J. Davis, R.L. Haedrich, L.-T. Tam and A.F. Riggs, Biochim. Biophys. Acta 870 (1986) 552.

2 J.M. Friedman, D.L. Rousseau and M.R. Ondrias, Annu. Rev. Phys. Chem. 33 (1982) 471.

3 J.M. Friedman, Science 228 (1985) 1273.
4 J.M. Friedman and B.F. Campbell, in: Protein structure: Molecular and electronic reactivity, ed. R. Austin (Springer, Berlin, 1987) p. 211.
5 D.L. Rousseau and J.M. Friedman, in: Biological applications of Raman spectroscopy, ed. T.G. Spiro (Wiley, New York, 1988) vol. 3, p. 133.
6 T. Kitagawa, in: Biological applications of Raman spectroscopy, ed. T.G. Spiro (Wiley, New York, 1988) vol. 3, p. 100.
7 J.M. Friedman, D.L. Rousseau, M.R. Ondrias and R.A. Stepnoski, Science 218 (1982) 1244.
8 M.R. Ondrias, D.L. Rousseau, J.A. Shelnutt and S.R. Simon, Biochemistry 21 (1982) 3428.
9 O. Bangcharvenpanpong, K.T. Schomacker and P.M. Champion, J. Am. Chem. Soc. 106 (1984) 5688.
10 M.F. Perutz, B. Shaanan and R.C. Liddington, Acc. Chem. Res. 20 (1987) 309.
11 M. Sassaroli, S. Dasgupta and D.L. Rousseau, J. Biol. Chem. 261 (1986) 376.
12 L. Powers, B. Chance, M. Chance, B. Campbell, J.M. Friedman, A. Naqui, K.S. Reddy and Y. Zhow, Biochemistry 26 (1987) 4785.
13 J.M. Friedman and M.R. Ondrias, Proc. SPIE 1055 (1989) 216.
14 A. Ansari, J. Berendzen, D. Braunstein, B.R. Cowen, H. Frauenfelder, M.K. Hong, I.E.T. Iben, J.B. Johnson, P. Ormos, T.B. Sauke, R. Scholl, A. Schulte, P.J. Steinbach, J. Vittitow and R.D. Young, Biophys. Chem. 26 (1987) 337.
15 J.M. Friedman, T.W. Scott, R.A. Stepnowski, M. Ikeda-Saito and T. Yonetani, J. Biol. Chem. 258 (1983) 10564.
16 S.D. Carson, C.A. Wells, E.W. Findsen, J.M. Friedman and M.R. Ondrias, J. Biol. Chem. 262 (1987) 3044.
17 K. Nagai and T. Kitagawa, Proc. Natl. Acad. Sci. U.S.A. 77 (1980) 2033.
18 K. Nagai, T. Kitagawa and H. Morimoto, J. Mol. Biol. 136 (1980) 271.
19 N. Shibayama, H. Morimoto and T. Kitagawa, J. Mol. Biol. (1986) 192.
20 M.R. Ondrias, D.L. Rousseau, T. Kitagawa, T. Ikeda-Saito, T. Inubushi and T. Yonetani, J. Biol. Chem. 257 (1982) 8766.
21 J.M. Friedman, D.L. Rousseau and F. Adar, Proc. Natl. Acad. Sci. U.S.A. 74 (1977) 2607.
22 W.R. Scheidt and D.M. Chipman, J. Am. Chem. Soc. 108 (1986) 1163.
23 M. Chance, L. Parkhurst, L. Powers and B. Chance, J. Biol. Chem. 261 (1986) 5689.
24 B.R. Gelin, A.W.M. Lee and M. Karplus, J. Mol. Biol. 171 (1986) 489.
25 M. Chavez, M. Chance, S. Courtney, J.M. Friedman and M.R. Ondrias, Biochemistry (1990) in the press.
26 B.F. Campbell, M. Chance and J.M. Friedman, Science 238 (1988) 373.
27 E.W. Findsen, T.W. Scott, M.R. Chance, J.M. Friedman and M.R. Ondrias, J. Am. Chem. Soc. 107 (1985) 3355.
28 M. Sassaroli and D.L. Rousseau, Biochemistry 26 (1987) 3092.
29 S.M. James, G.A. Nalickas, W.A. Eaton and R.M. Hochstrasser, Biophys. J. 54 (1988) 545.
30 T.W. Scott and J.M. Friedman, J. Am. Chem. Soc. 106 (1984) 5677.
31 J.M. Friedman and B.F. Campbell, Spectroscopy 1 (1986) 34.
32 S. Matsukawa, K. Mawatari, Y. Toneyama and T. Kitagawa, J. Am. Chem. Soc. 105 (1985) 1108.
33 V. Srajer, L. Reinisch and P.M. Champion, J. Am. Chem. Soc. 110 (1988) 6656.
34 E.W. Findsen, J.M. Friedman, M.R. Ondrias and S.R. Simon, Science 229 (1985) 661.
35 M. Tsubaki and N.-T. Yu, Biochemistry 21 (1982) 1140.
36 D.L. Rousseau, S.L. Tan, M.R. Ondrias, S. Ogawa and R.W. Noble, Biochemistry 23 (1984) 2857.
37 B.D. Olafson and W.A. Goddard, III, Proc. Natl. Acad. Sci U.S.A. 74 (1977) 1315; W.A. Goddard, III and B.D. Olafson, in: Biochemical and chemical aspects of oxygen, ed. W. Caughy (Academic Press, New York, 1979) p. 87.
38 B.R. Gelin and M. Karplus, Proc. Natl. Acad. Sci. U.S.A. 74 (1977) 801.
39 T. Iizuka, H. Yamamoto, M. Kotani and T. Yonetani, Biochim. Biophys. Acta 371 (1974) 126.
40 J.M. Friedman, R.A. Stepnoski and R. Noble, FEBS Lett. 146 (1982) 278.
41 R.H. Austin, K.W. Beeson, L. Eisenstein, H. Frauenfelder and I.C. Gunsalus, Biochemistry 14 (1975) 5355.
42 J.M. Friedman, T.W. Scott, G.J. Fisanick, S.R. Simon, E.W. Findsen, M.R. Ondrias and V.W. MacDonald, Science 229 (1985) 187.
43 L.P. Murray, J. Hofrichter, E.R. Henry, M. Ikeda-Saito, K. Kitageshi, T. Yonetani and W.A. Eaton, Proc. Natl. Acad. Sci. U.S.A. 85 (1988) 2151.
44 J.M. Friedman, S.R. Simon and T.W. Scott, Copeia 3 (1985) 679.